Electronic Supplementary Material (ESI) for Physical Chemistry Chemical Physics.

Supporting Information

Photoinduced Charge Recombination in Dipolar D-A-A Photonic Liquid Crystal Polymorphs

Mercedes M. A. Mazza[†], Shiori Yamazaki[†], Dieu X. Mai[†], Suyog Padgaonkar[†], Samuel Peurifoy[†], Ariane Goncalves[†], Yi-Lin Wu[‡], Qiaoyu Hu[†], and Amy M. Scott[†]*

[†]*Department of Chemistry, University of Miami, 1301 Memorial Drive, Coral Gables, FL 33146*

[‡]*Department of Chemistry, Northwestern University, Evanston, IL 60208*

*amscott@miami.edu

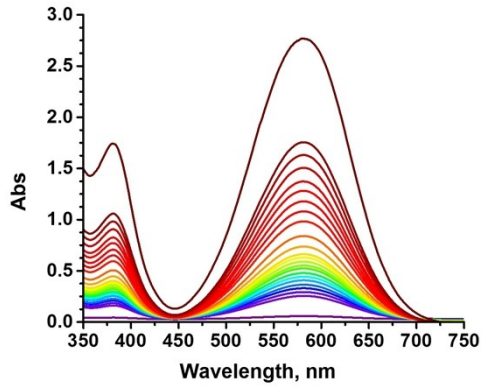

Figure S1. Titration of **C6-TPA-BT-CN** in toluene perfomed by UV/VIS spectroscopy.

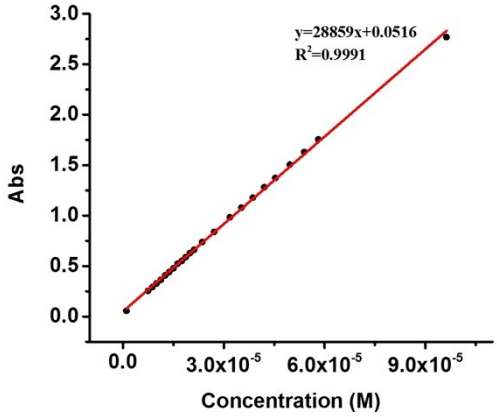

Figure S2. Plot of the measured absorbance at increasing concentration of **C6-TPA-BT-CN** in toluene.

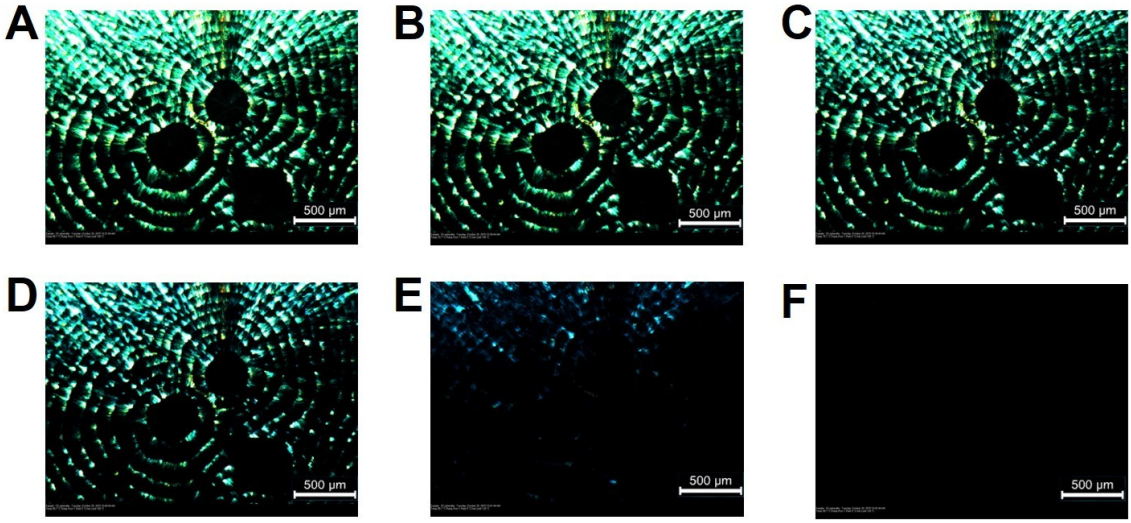

Figure S3. PLM images of **C6-TPA-BT-CN** drop-cast film (banded spherulite spot) as a function of temperature with processing solvent chlorobenzene. **A**, 65.7 °C. **B**, 70.7 °C. **C**, 75.7 °C. **D**, 80.7 °C. **E**, 85.7 °C. **F,** 90.7 °C.

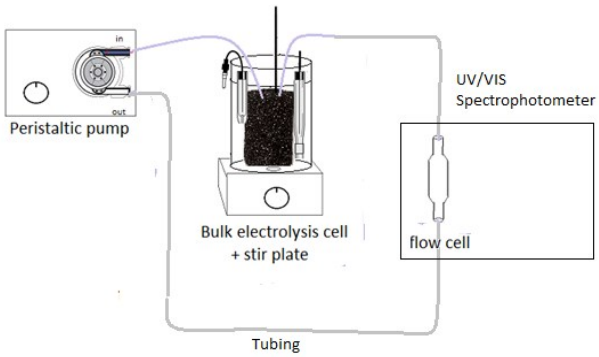

Figure S4. The set-up for bulk electrolysis.

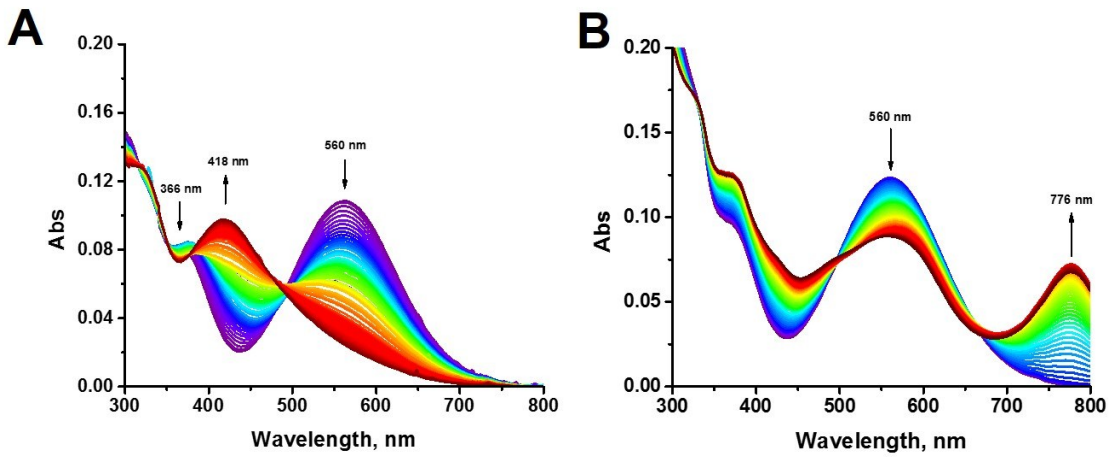

Figure S5. Electrochemical UV-Vis spectrum of **C6-TPA-BT-CN** during oxidation with 0.1M NBu_4PF_6 as the supporting electrolyte in DMSO at +1.5V **(A)** and +1V **(B)** (vs. Ag/AgCl).

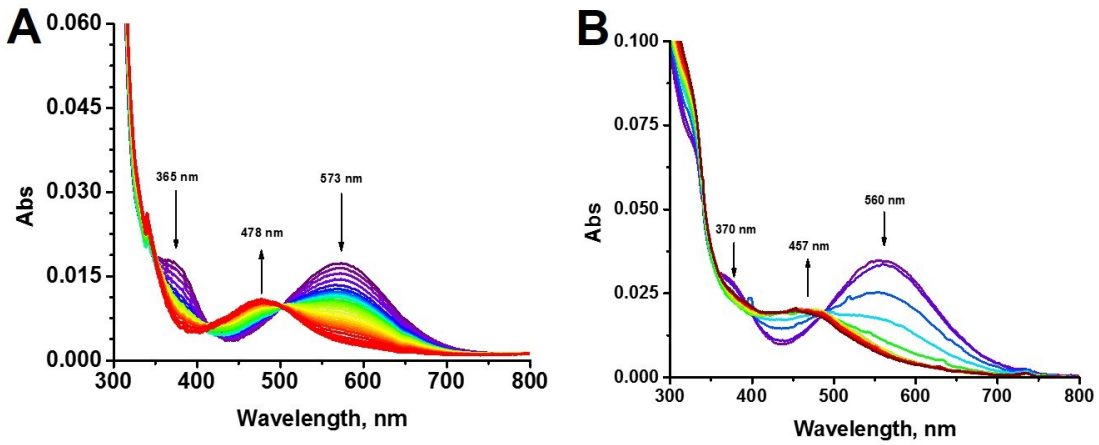

Figure S6. Electrochemical UV-Vis spectrum of **C6-TPA-BT-CN** during reduction with 0.1M NBu_4PF_6 as the supporting electrolyte in THF at -0.1V **(A)** and -1V **(B)** (vs. Ag/AgCl).

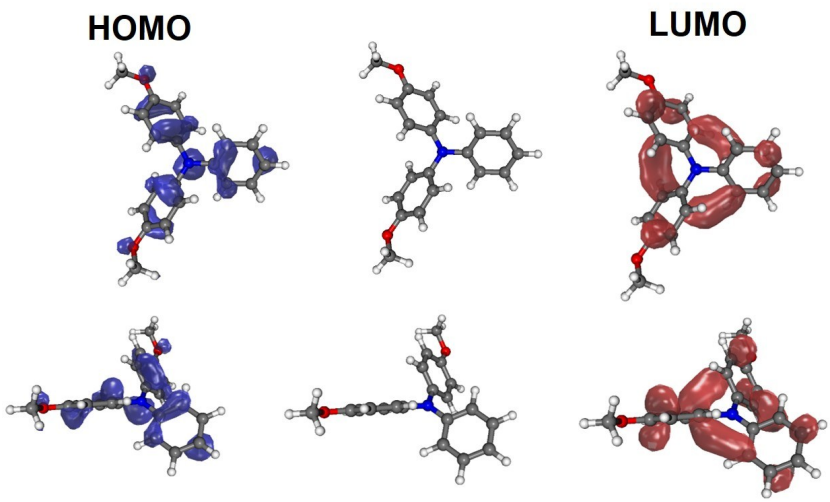

Figure S7. Visualization of the HOMO (left) and LUMO (right) of N,N-bis(4-methyloxyphenyl)phenylamine **C1-TPA**.

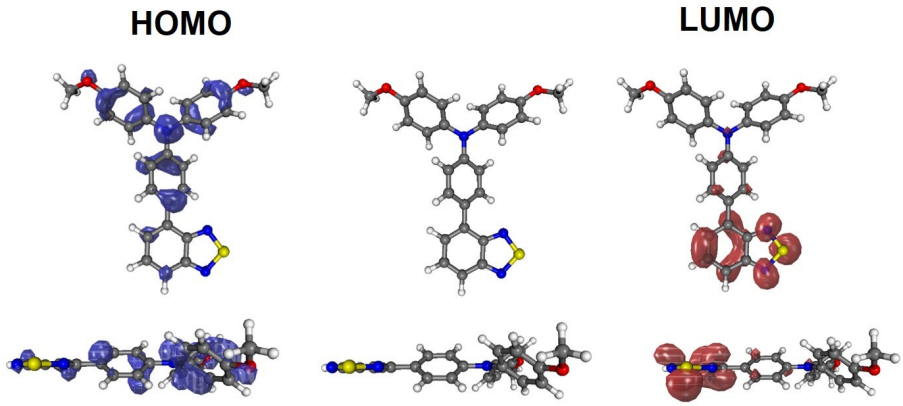

Figure S8. Visualization of the HOMO (left) and LUMO (right) of [N,N-bis(4-methyloxyphenyl)amino]phenyl)-2,1,3-benzothiadiazole **C1-TPA-BT**.

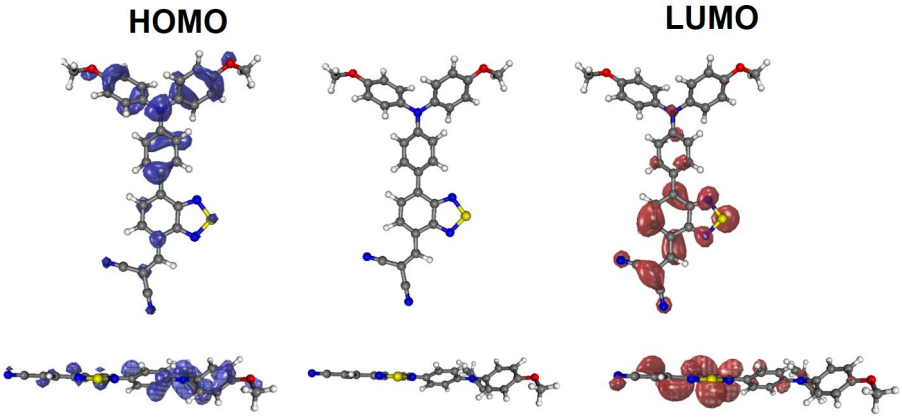

Figure S9. Visualization of the HOMO (left) and LUMO (right) of N,N-bis(4-methyloxyphenyl)amino]phenyl)-2,1,3-benzothia-diazol-4-yl)methylene]propane-dinitrile **C1-TPA-BT-CN**.

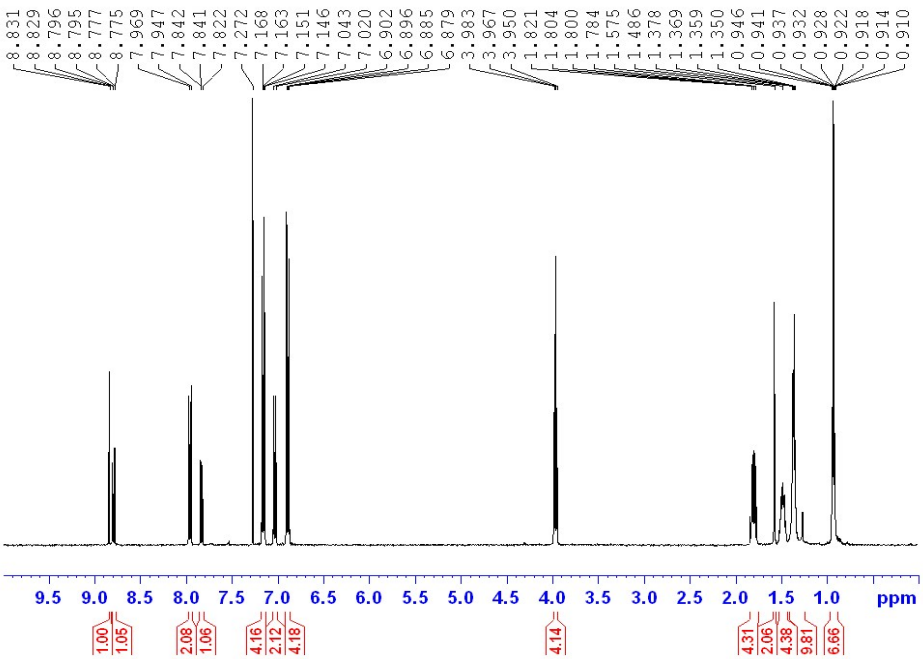

Figure S10. ^{1}H NMR spectrum of **C6-TPA-BT-CN** in $CDCl_3$ at room temperature

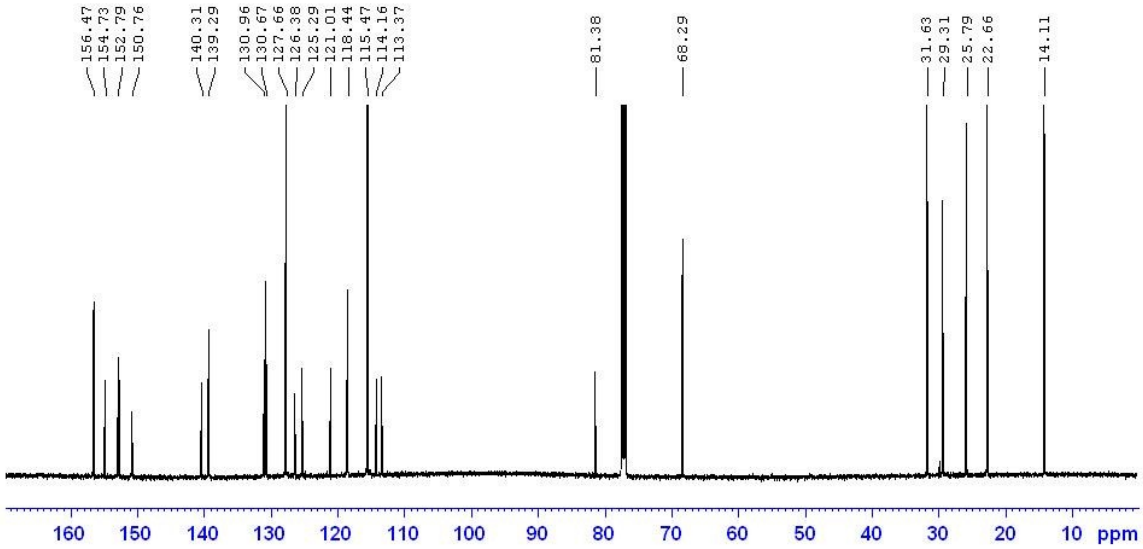

Figure S11. ^{13}C NMR spectrum of **C6-TPA-BT-CN** in $CDCl_3$ at room temperature

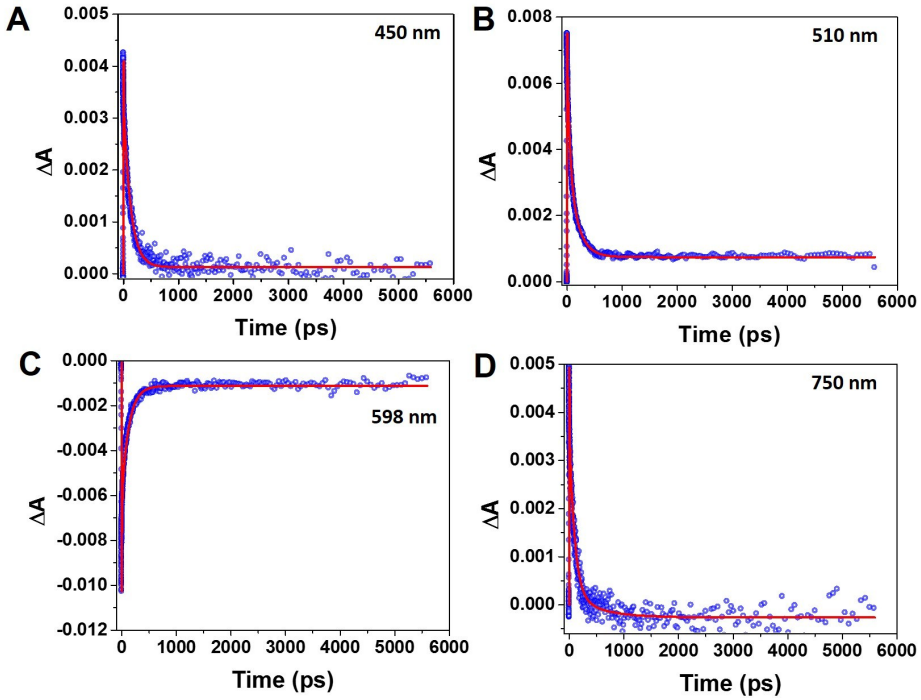

Figure S12. Kinetics at (A) 450 nm, (B) 510 nm, (C) 598 nm and (D) 750 nm, relative to fs-TA spectra of C_6TBTCN amorphous film upon 400 nm excitation (200 nJ/pulse, 1.58 x 10^{-4} J/cm^2).

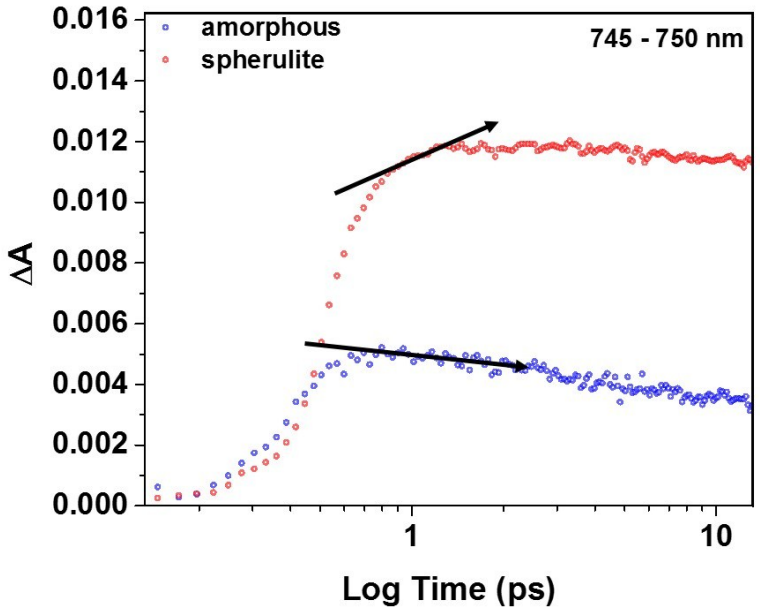

Figure S13. Comparison of the Abs vs Log time of selected kientic trace of amorphous (blue) and spherulite (red) films.

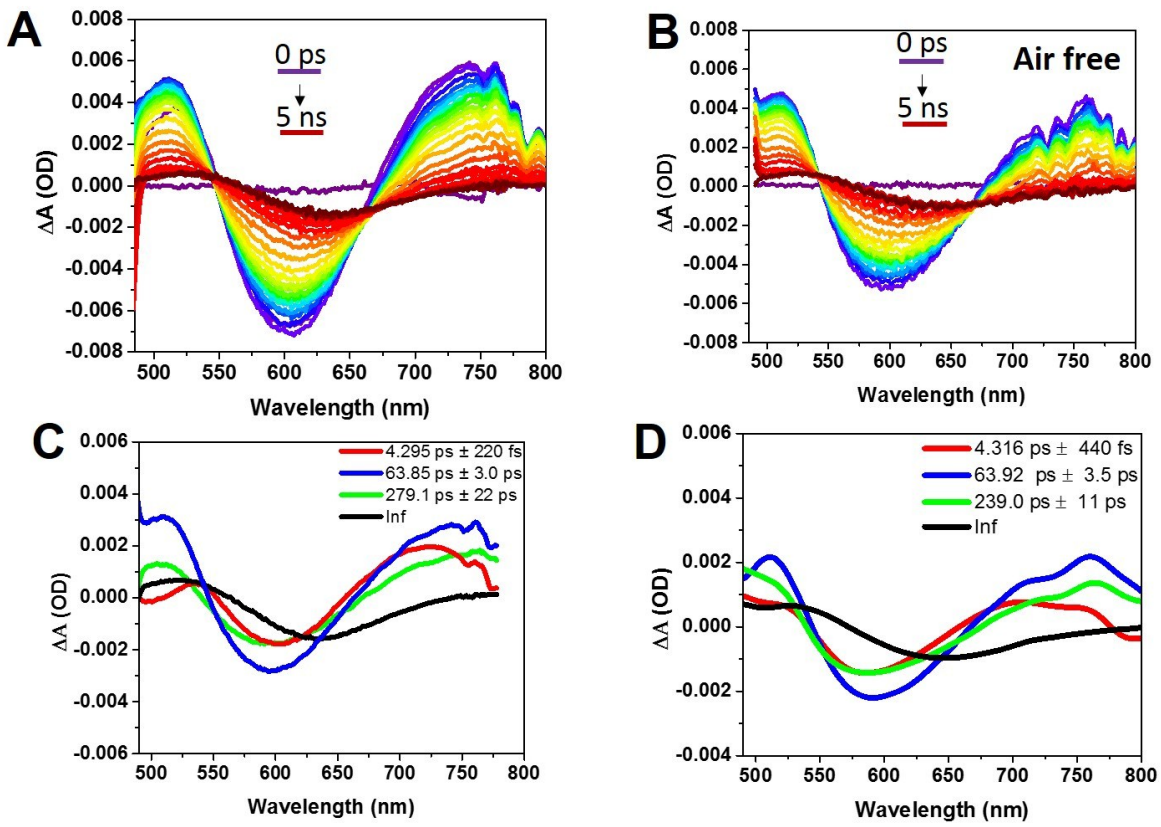

Figure S14. FsTA of C6-TPA-BT-CN amorphous films in air A) and air free B) upon 470 nm photoexcitation. Global fit analysis of the photoinduced dynamics of C6-TPA-BT-CN amorphous films in air C) and air free D).

Calculated Frontier Molecular Orbital Energy Levels						
	Singlet State			**Triplet State**		
Molecule	**HOMO** (eV)	**LUMO** (eV)	**Bandgap** (eV)	**HOMO** (eV)	**LUMO** (eV)	**Bandgap** (eV)
C1-TPA	-4.8666	-0.9962	3.8704	-1.1768	-0.2091	0.9677
C1-TPA-BT	-4.8763	-2.3125	2.5638	-2.8287	-0.7694	2.0593
C1-TPA-BT-CN	-4.9894	-3.0731	1.9163	-3.7195	-1.5555	2.1640

Table S1. Frontier Molecular Orbital Values from Calculations

C_6-TPA-BT-CN in toluene – individual fit				
$\lambda_{exc.}$ 400 nm VIS	τ_{rise} (ps)	A_r %	τ_1 (ps)	A_1 %
480-700	4.6 ± 0.9	100	119.4 ± 0.7	100

Table S2. Kinetic data obtained from multiwavelegth analysis (average over 6 wavelengths from 480 to 700 nm) of FsTA spectra of the **C6-TPA-BT-CN** in toluene, where τ are lifetimes and A the corresponding amplitudes.

C6-TPA-BT-CN amorphous – individual fit								
$\lambda_{exc.}$ 400 nm VIS	τ_1(ps)	A_1 %	τ_2 (ps)	A_2 %	τ_3 (ps)	A_3 %	τ_4 (ns)	A_4 %
(A) 450	2.8 ± 0.1	24	-	-	130.5 ± 1.4	74	> 6	2
(B) 510	6.8 ± 0.3	12	43.0 ± 3.2	36	164.4 ± 7.8	40	> 6	12
(C) 598	1.6 ± 0.2	27	30.4 ± 5.3	24	174.7 ± 17.1	35	> 6	14
(D) 750	3.8 ± 0.3	27	87.2 ± 6.2	55	503.33 ± 6.6	12	> 6	6

Table S3. Kinetic data obtained from individual wavelengths analysis (representative of the four characteristic peaks (a, b, c, and d) of fs-TA spectra of the **C6-TPA-BT-CN** amorphous film, where $\tau_{1\text{-}4}$ are lifetimes and $A_{1\text{-}4}$ the corresponding amplitudes. Note that a fourth lifetime component is observed in all the kinetic fits exceeding the limits of our setup (5.5 ns).

S1. General Methods

A Pure Solv MD-6 solvent purification system was used to dry all solvents. All starting materials and reagents were purchased from commercial sources (VWR or Aldrich Chemicals) and used without further purification unless otherwise noted. The synthetic route of molecule **4** was modified based on the previously reported methods[1, 2]. Column chromatography purifications were done by using the Sigma-Aldrich high-purity grade silica gel (60 Å, 230-400 mesh size). Aluminum sheets precoated with silica gel 60 (EMD 40-60 mm, 230-400 mesh with 254 nm dye) were applied for thin layer chromatography (TLC). TLC plates were visualized by ultraviolet (UV) light. All reactions were performed under an inert argon atmosphere with standard Schlenk line techniques unless otherwise noted. ^{1}H and ^{13}C NMR spectra were obtained by a Bruker AVANCE 400 and 500 MHz spectrometer. Deuterated chloroform ($CDCl_3$) was used as the solvent for all NMR samples. Chemical shifts were reported in δ units with the solvent residual peak as the internal standard. The following abbreviations are used for signal multiplicities: s (singlet), d (doublet), t (triplet), q (quartet), m (multiplet). Electrospray Ionization Mass Spectra (ESI-MS) were performed on an Agilent LC/MSD Trap XCT system. An Agilent 6200 LC/MSD TOF system was used to obtain high resolution mass spectra. UV-Vis absorption spectra were collected by a Shimadzu 1800 UV spectrometer. The fluorescence measurements were done on a Shimadzu RF-5301 PC spectrofluorophotometer. Standard drop-casting techniques were applied to make thin films for further measurements. Polarized optical microscopy (POM) images were taken by a Leica DM2700 P microscope with a 530 nm polarizer and a 10x objective. Atomic force microscopy (AFM) characterizations were performed on a Park System XE 150 Scanning probe microscope using Nanosensors™ PPP NCHR probes under non-contact mode.
The laser facility in the Scott Laboratory includes two 5'x10' Spectra-Physics Smart air tables with additional damping controllers, and a Spectra Physics 35-fs titanium sapphire laser (800 nm output) (Spectra-Physics Mai Tai Oscillator, 84 MHz, and 5W Spitfire Ace Amplifier pumped by a 527 nm Nd:YLF Empower laser) operating at 1 and 5 kHz and pumps an optical parametric amplifier (OPA, Spectra Physics, Topas) to produce excitation pulses ranging from 290 nm - 2600 nm with an instrument response time of ~ 150 fs. The laser lab is also equipped with a commercial transient absorption detection system, Helios spectrometer from Ultrafast Systems, that collects spectra in the visible range (300 - 800 nm) and near-infrared (800 - 1400 nm) from 35 fs to approximately 6 ns, along with a EOS nanosecond attachment that collects data from ~ 1 ns to microseconds in both the visible and near-infrared[3].

S2. Synthesis

Overall Synthetic Scheme

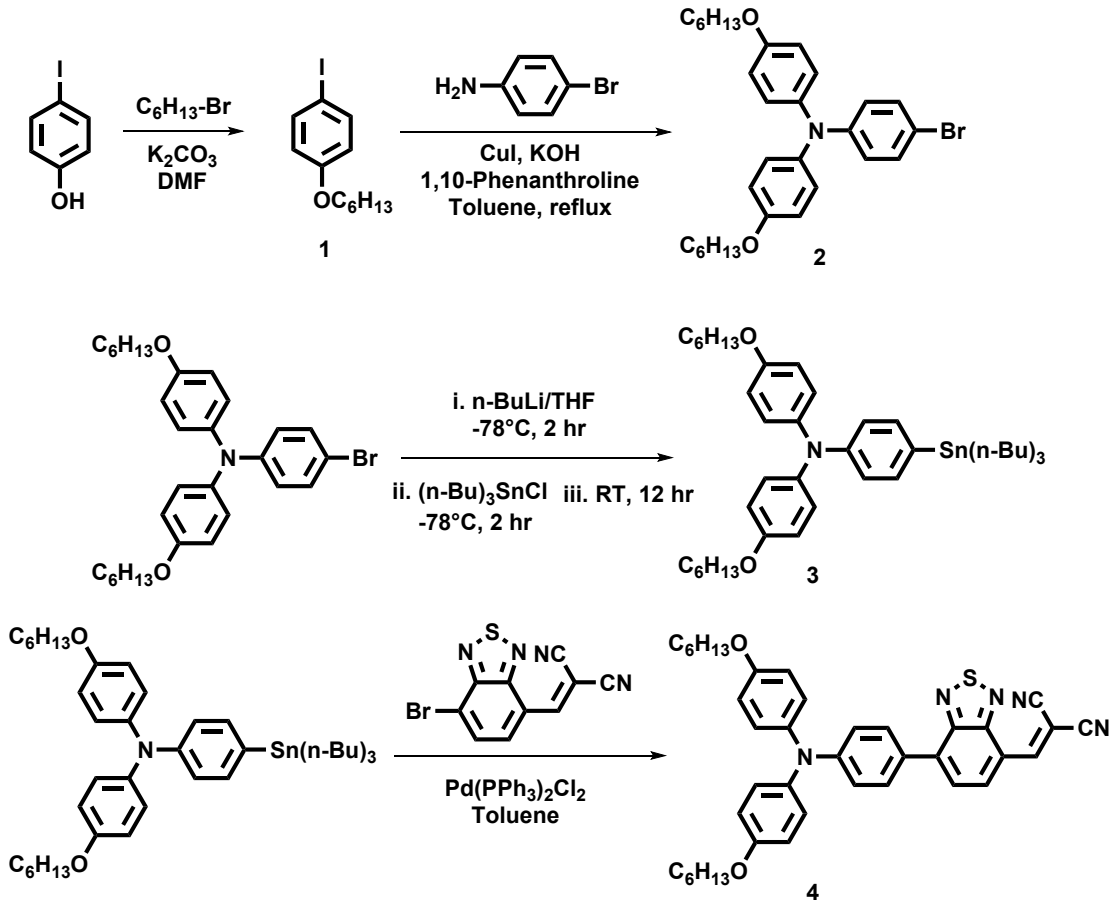

Scheme S1. Preparation of **4**.

1-hexyloxy-4-iodobenzene (1): K_2CO_3 (3.8 g, 27.5 mmol) was added to a suspension of 4-iodophenol (5.0 g, 22.7 mmol), 1-bromohexane (4.12 g, 25.0 mmol), and DMF (60 mL) under argon. After being stirred at 150 °C under reflux for 24h, the mixture was filtered. The crude product was extracted into methylene chloride, washed with water, and dried over anhydrous magnesium sulfate ($MgSO_4$). After removing solvent under reduced pressure, the residue was purified by column chromatography (SiO_2, petroleum ether) to yield a colorless oil (90%). ^{1}H NMR (500 MHz, $CDCl_3$, 25℃): δ 7.54 (d, 2H), 6.67 (d, 2H), 3.91 (t, 2H), 1.81-1.55 (m, 2H), 1.47-1.25 (m, 6H), 0.90 (t, 3H).

N,N-bis(4-hexyloxyphenyl)-4-bromophenylamine (2): **1** (6.185 g, 20.35 mmol), 4-bromoaniline (1.4 g, 8.14 mmol), cuprous iodide (0.155 g, 0.814 mmol), 1,10-phenanthroline (0.147 g, 0.816 mmol), potassium hydroxide flakes (7.29 g, 0.130 mol), and toluene (40 mL) were added to a 250mL round-bottomed flask equipped with a magnetic stirrer and a Dean-Stark trap under a reflux jacketed condenser. The reaction mixture was rapidly heated over a period of 30 min to 125 °C and maintained at this temperature under argon for 24 h. After cooling to room temperature, the mixture was diluted with dichloromethane and washed with 1 M HCl and brine before being dried over anhydrous $MgSO_4$. The crude product was purified by column chromatography (SiO_2, 1:10 DCM:petroleum ether) to produce a colorless oil (60%). ^{1}H NMR (500 MHz, $CDCl_3$, 25℃): δ 7.26 (d, 2H), 7.05 (d, 4H), 6.87-6-80 (m, 6H), 3.96 (t, 4H), 1.86-1.77 (m, 4H), 1.51-1.33 (m, 12H), 0.93 (t, 6H).

4-(N,N-bis(4-hexyloxyphenyl)-1-(tri-n-butylstannyl)phenylene (3): n-BuLi (2.5 M in hexane, 1.05 mL, 2.66 mmol) was added drop-wise to a solution of **2** (1.27 g, 2.42 mmol) in 20 mL of THF at -78°C under argon. After the mixture was stirred for 2 h, tributylstannyl chloride (0.78 mL, 2.88 mmol) was added to the mixture, and the mixture was maintained at -78°C and stirred for another 2 h. Then slowly warmed the mixture to room temperature and stirred for 12 - 15 h. After reaction, the mixture was poured into water and extracted with diethyl ether. The organic extracts were then dried over anhydrous $MgSO_4$. Upon evaporation of the solvent, the crude product was obtained for the next step (**4**) without further purification.

4-(N,N-bis(4-hexyloxyphenyl)-1-(7-dicyanovinyl-2,1,3-benzothiadiazole)phenylene (4) (C_6-TPA-BT-CN): A mixture of 4-bromo-7-dicyanovinyl-2,1,3-benzothiadiazole (100 mg, 0.343 mmol), **3** (302 mg, 0.411 mmol), and $PdCl_2(PPh_3)_2$ (12 mg, 0.017 mmol) in anhydrous toluene (10 mL) was stirred and heated to 110 °C under argon for 5 h. After the reaction mixture was cooled to room temperature, transfer it into a separation funnel and add deionized water. The separated toluene layer was again washed with dilute potassium fluoride (KF) solution twice. Then the toluene layer was filtered and washed with toluene. The solvent was removed by rotary evaporation, and the crude product was purified by column chromatography (SiO_2, 1:1 DCM:hexane) to afford a blue sticky solid (20%). ^{1}H NMR (500 MHz, $CDCl_3$, 25℃): δ 8.85 (s, 1H), 8.88 (d, 1H), 7.98 (d, 2H), 7.85 (d, 1H), 7.18 (d, 4H), 7.02 (d, 2H), 6.9 (d, 4H), 3.96 (t, 4H), 1.86-1.77 (m, 4H), 1.50 (m, 4H), 1.48-1.33 (m, 8H), 0.93 (t, 6H). ^{13}C NMR (500 MHz, $CDCl_3$, 25℃): δ 156.47, 154.73, 152.79, 150.76, 140.31, 139.29, 130.96, 130.67, 127.66, 126.38, 125.29,

121.01, 118.44, 115.47, 114.16, 113.37, 81.38, 68.29, 31.63, 29.31, 25.79, 22.66, 14.11. ESI-MS: Calculated 655.86, Found: 656.30.

S3. Solution Aggregation Study

In order to study the aggregation state of C6-TPA-BT-CN in solution, the titration measurements were performed on a Shimadzu 1800 UV spectrometer. Illustrated by the Figure S1 and S2, as the concentration of the molecule in solution increased, the UV absorbance increased linearly, indicating that the C6-TPA-BT-CN molecules exist as dispersed state rather than aggregated state. According to the Beer-Lambert Law ($A = \varepsilon CL$), the molar extinction coefficient (28859 $cm^{-1}M^{-1}$) could be obtained from the slope of Abs. vs Con. (Figure S2).

S4. Polarized Light Microscopy (PLM)

In Figure S3 is shown the PLM images of C6-TPA-BT-CN banded spherulite film on drop-cast film as a function of temperature. As the temperature increased, the film gradually changed from crystalline phase (A) to liquid crystal phase and finally to isotropic liquid phase (F), which displayed no birefringence, as supported by the dark image obtained under crossed polarized light.

S5. Cyclic Voltammetry and Spectroelectrochemistry

An electrochemical workstation (CH instruments, CHI 660) was used to control the potential and convert the current signal to the potential signal in cyclic voltammetry (CV) and spectroelectrochemistry experiments. Cyclic voltammograms were obtained by using a polished glassy carbon working electrode, a Pt wire counter electrode, and a Ag/AgCl reference electrode. The molecule was dissolved in tetrahydrofuran (THF) with with 0.1 M tetrabutylammonium hexafluorophosphate (NBu_4PF_6), as the supporting electrolyte. Before each measurement, the THF-saturated Ar was purged into the sample. Figure S4 shows the set-up figure of spectroelectrochemistry (bulk electrolysis), which, together with the UV-Vis spectrometer, was used to determine the spectral signatures of the radical cation (Figure S5) and anion (Figure S5) of C6-TPA-BT-CN. In bulk electrolysis, the reference electrode and the counter electrode were the same as those used in the CV, except that the working electrode was composed of Reticulated Vitreous Carbon (RVC) whose area is roughly 400cm^2. Dimethyl sulfoxide (DMSO) was used as the solvent with 0.1 M NBu_4PF_6 as the supporting electrolyte. Before each measurement, the dried Ar was purged into the sample. The solution was stirred when the experiment was running. A Teflon cap was employed to prevent air from entering the solution when argon or nitrogen was flowing through the cell. A peristaltic pump was applied to drive the solution flowing through the silicone tube.

S6. Computational Analysis

In the computational analysis, the long side chain attached on the oxygen atom was substituted by methyl group. From the visualization of the HOMO and LUMO of these three molecules, it can be derived that the HOMO is localized on the triphenylamine (TPA) moiety while the LUMO is localized on the anchoring group. The π-conjugated linker should play an essential role in CT process and has a significant effect on the photophysical property of the D-A-A system[4]. To understand the effect of building up a D-A-A structure, computational calculations have been conducted (Figure S7, S8, S9). As summarized in Table S1, as the donor-acceptor-acceptor (D-A-A) system is built, the HOMO energy level and bandgap of the molecule become deeper lying and smaller, respectively, which are beneficial to increase the open circuit voltage (V_{oc}) of solar cell device and absorb more solar ligh[5].

S7. NMR

Figure S10 and S11 show, respectiveli the ^{1}H NMR spectrum and the ^{13}C NMR spectrum of C6-TPA-BT-CN in $CDCl_3$ at room temperature.

S8. Transient Absorption Spectroscopy

Femtosecond transient absorption (FsTA) measurements were performed with an instrument based on a commercial amplified Ti:sapphire laser system (Spectra-Physics Mai Tai Oscillator (80MHz) and 5W Spitfire Ace Amplifier pumped by a 527 nm Nd:YLF Empower laser) operating at 1 kHz and pumps an optical parametric amplifier (OPA), Spectra Physics, Topas) to produce excitation pulse at 400 nm and 470 nm. Three different powers were used, 400 and 1200 nJ/pulse for solution state experiments and 200 nJ/pulse for solid state experiments. The pump beam diameter was 0.4 mm resulting in energy densities of 1.58 x 10^{-4} J/cm^2 (for 200 nJ/pulse), 3.18 x 10^{-4} J/cm^2 (for 400 nJ/pulse) and 9.55 x 10^{-4} J/cm^2 (for 1200 nJ/pulse) on neat films. The data were collected through a Helios spectrometer (Ultrafast System) in which the probe is delayed relative to te pump on a mechanical delay line. The pump beam is chopped at half the repetition rate of the laser, so that the absorption change (ΔA) can be measured as a function of delay time, where $\Delta A = - \log (I_{pump + probe} II_{probe})$. The data were background subtracted, chirp-corrected using the Ultrafast System Surface Xplorer Software over the spectral range in the visible region. Table S2 and S3 summarize the FsTA kinetic data obtained for C6-TPA-BT-CN in toluene and amorphous films, where τ are lifetimes and A the corresponding amplitudes. In Figure S12 are shown the individual kinetics at (A) 450 nm, (B) 510 nm, (C) 598 nm and (D) 750 nm, relative to FsTA spectra of C6-TPA-BT-CN amorphous film upon 400 nm excitation (200 nJ/pulse, 1.58 x 10^{-4} J/cm^2). In Figure S14 is shown the comparison between the fsTA spectra and global fit analysis of C6-TPA-BT-CN amorphous films in air and air free conditions.

9. References

1. Y. H. Chen, L. Y. Lin, C. W. Lu, F. Lin, Z. Y. Huang, H. W. Lin, P. H. Wang, Y. H. Liu, K. T. Wong, J. Wen, D. J. Miller and S. B. Darling, *J Am Chem Soc*, 2012, **134**, 13616-13623.
2. L. Y. Lin, Y. H. Chen, Z. Y. Huang, H. W. Lin, S. H. Chou, F. Lin, C. W. Chen, Y. H. Liu and K. T. Wong, *J Am Chem Soc*, 2011, **133**, 15822-15825.
3. C. X. Guzman, R. M. K. Calderon, Z. Li, S. Yamazaki, S. R. Peurifoy, C. Guo, S. K. Davidowski, M. M. A. Mazza, X. Han, G. Holland, A. M. Scott and A. B. Braunschweig, *The Journal of Physical Chemistry C*, 2015, **119**, 19584-19589.
4. A. M. Scott and M. R. Wasielewski, *J Am Chem Soc*, 2011, **133**, 3005-3013.
5. H. Xin, S. Subramaniyan, T.-W. Kwon, S. Shoaee, J. R. Durrant and S. A. Jenekhe, *Chemistry of Materials*, 2012, **24**, 1995-2001.